Inorg. Chem. **2006**, *45*, 5924–5937

Synthesis, Characterization, Reactivity, and Catalytic Potential of Model Vanadium(IV, V) Complexes with Benzimidazole-Derived ONN Donor Ligands

Mannar R. Maurya,*,† Amit Kumar,† Martin Ebel,‡ and Dieter Rehder*,‡

Department of Chemistry, Indian Institute of Technology Roorkee, Roorkee 247 667, India, and Institut für Anorganische und Angewandte Chemie, Universität Hamburg, Martin-Luther-King-Platz 6, 20146 Hamburg, Germany

Received March 23, 2006

Reaction between $[VO(acac)_2]$ and the ONN donor Schiff base Hsal-ambmz (**I**) (Hsal-ambmz = Schiff base obtained by the condensation of salicylaldehyde and 2-aminomethylbenzimidazole) resulted in the formation of the complexes $[V^{IV}O(acac)$(sal-ambmz)] (**1**), $[V^{V}O_2$(acac-ambmz)] (**2**) (Hacac-ambmz = Schiff base derived from acetylacetone and 2-aminomethylbenzimidazole), and the known complex $[V^{IV}O$(sal-phen)] (**3**) (H_2sal-phen = Schiff base derived from salicylaldehyde and *o*-phenylenediamine). Similarly, $[V^{IV}O(acac)$(sal-aebmz)] (**7**) has been isolated from the reaction with Hsal-aebmz (**II**) (Hsal-aebmz derived from salicylaldehyde and 2-aminoethylbenzimidazole). Aerial oxidation of the methanolic solutions/suspensions of **1** and **7** yielded the dioxovanadium(V) complexes $[V^{V}O_2$(sal-ambmz)] (**4**) and $[V^{V}O_2$(sal-aebmz)] (**8**), respectively. Reaction of $VOSO_4$ with **II** gave $[\{V^{IV}O$(sal-aebmz)$\}_2SO_4]$ (**9**) and $[V^{IV}O$(sal-aebmz)$_2]$ (**10**), along with **3** and **8**. Under similar reaction conditions, **I** gave only $[\{V^{IV}O$(sal-ambmz)$\}_2$-$SO_4]$ (**5**) and **3** as major products. Treatment of **1** and **7** with benzohydroxamic acid (Hbha) yielded the mixed-chelate complexes $[V^{V}O$(bha)(sal-ambmz)] (**6**) and $[V^{V}O$(bha)(sal-aebmz)] (**11**). The crystal and molecular structures of **2**, **3**·1/2DMF, **7**·1/4H_2O, **8**, **9**·2H_2O, **10**, and **11** have been determined, confirming the ONN binding mode of the ligands. In complex **10**, one of the ligands is coordinated through the azomethine nitrogen and phenolate oxygen only, leaving the benzimidazole group free. In the dinuclear complex **9**, bridging functions are the phenolate oxygens from both of the ligands and two oxygens of the sulfato group. The unstable oxoperoxovanadium(V) complex $[V^{V}O(O_2)$(sal-aebmz)] (**12**) has been prepared by treatment of **7** with aqueous H_2O_2. Acidification of methanolic solutions of **7** and **10** lead to (reversible) protonation of the bemzimidazole, while **8** was converted to an oxo-hydroxo species. Complexes **2**, **4**, and **8** catalyze the oxidation of methyl phenyl sulfide to methyl phenyl sulfoxide and methyl phenyl sulfone, a reaction mimicking the sulfideperoxidase activity of vanadate-dependent haloperoxidases. These complexes are also catalytically active in the oxidation of styrene to styrene oxide, benzaldehyde, benzoic acid, and 1-phenylethane-1,2-diol.

Introduction

Interest in the coordination chemistry with particular emphasis on the model character of vanadium(V) complexes having O and N functionalities[1] stems from the structural characterization of three vanadate-dependent haloperoxidases (VHPO). Irrespective of their origin from brown algae (*Ascophyllum nodosum*),[2] red algae (*Corallina officinalis*),[3] or fungi (*Curvularia inequalis*),[4] they all show a high degree of amino acid homology in their active centers and have almost identical structural features, with vanadium(V) in a trigonal-bipyramidal coordination environment. Vanadium is covalently linked to three nonprotein oxo groups in the

* To whom correspondence should be addressed. E-mail: rkmanfcy@iitr.ernet.in. Tel: +91 1332 285327. Fax: +91 1332 173560.
† Indian Institute of Technology Roorkee.
‡ Universität Hamburg.

(1) (a) Butler, A.; Carrano, C. J. *Coord. Chem. Rev.* **1991**, *109*, 61−105. (b) Butler, A. *Coord. Chem. Rev.* **1999**, *187*, 17−25. (c) Rehder, D. *Coord. Chem. Rev.* **1999**, *182*, 297−322. (d) Rehder, D. In *Transition Metals in Biology and Their Coordination Chemistry*; Trautwein, A. X., Ed.; Wiley-VCH: Weinheim, 1997; pp 491−504. (e) Maurya, M. R. *Coord. Chem. Rev.* **2003**, *237*, 163−181. (f) Crans, D. C.; Smee, J. J.; Gaidamauskas, E.; Yang, L. *Chem. Rev.* **2004**, *104*, 849−902.
(2) Weyand. M.; Hecht, H. J.; Keiss, M.; Liaud, M. F.; Vilter, H.; Schomburg, D. *J. Mol. Biol.* **1999**, *293*, 595−611.

10.1021/ic0604922 CCC: $33.50 © 2006 American Chemical Society
Published on Web 06/24/2006

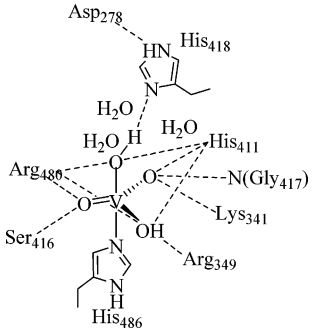

Figure 1. Active-site structure of vanadate-dependent haloperoxidase from *Ascophyllum nodosum* (in *Curvularia inequalis*, the His_{411} is replaced by Phe_{397}).

equatorial plane, to the protein backbone through N_ϵ of an imidazole moiety of a proximal histidine, and to an axial OH group trans to the histidine, further hydrogen bonded to a distal (catalytic) histidine and water molecules (Figure 1). These enzymes, as well as various model complexes, catalyze the oxidation, by peroxide, of halide to hypohalous acid[5] and of (prochiral) sulfides to (chiral) sulfoxides (eqs 1 and 2),[6] and of several other organic substrates.[7]

$$Hal^- + H_2O_2 + H^+ \rightarrow HOHal + H_2O \ (Hal^- = \text{halide}) \quad (1)$$

$$RSR' + H_2O_2 \rightarrow RS(O)R' + H_2O \quad (2)$$

Vanadium complexes containing imidazole or imidazole derivatives as ligands can be considered structural models of VHPO. The first structural characterization of an imidazolvanadium complex[8] was followed by reports on the characterization and reactivity of oxovanadium(IV) and (V) complexes containing the imidazole moiety.[9] Spectral changes observed for VO^{2+} complexes treated with acid suggested the protonation of either coordinated imidazole (in [VO(acac)(sal-im)] and [VO(sal)(sal-im)]) or noncoordinated imidazole (in [$VO(sal\text{-}im)_2$]) (H_2sal-im = 4-(2-(salicylideneamino)ethylimidazole) and were correlated to those observed for the reduced form of vanadate-dependent bromoperoxidase. Electron Spin−Echo Envelop Modulation (ESEEM) studies, however, suggested that the azomethine nitrogen of the Schiff base of [VO(acac)(sal-im)] is protonated and detached from vanadium upon addition of 1 equiv of acid.[10] In the histidine-derived dioxovanadium(V) complex [VO_2(naph-his)] (H_2naph-his = Schiff base derived from 2-hydroxy-1-naphthaldehyde and histidine), the imine nitrogen of the histidine moiety is protonated and thus not involved in coordination.[11] Oxovanadium(IV) and dioxovanadium(V) complexes reported by Crans et al., having the benzimidazole unit in the ligand system, provide models for the coordination of histidine in the enzyme.[12] Other complexes containing imidazole (or its derivatives) have also been described where the imidazole either acts as a co-ligand or, in its protonated form, as a counterion for the complex.[13]

Scheme 1

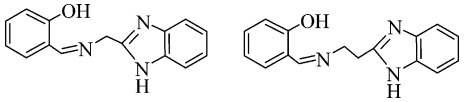

Hsal-ambmz (**I**) Hsal-aebmz (**II**)

In continuation of our efforts on the characterization of structural and functional models of VHPO,[14] we report here the syntheses of oxovanadium(IV), oxovanadium(V), and dioxovanadium(V) complexes of the benzimidazole-derived ligands **I** and **II** formed from salicylaldehyde (Hsal) and 2-aminomethylbenzimidazole (ambmz) or 2-aminoethylbenzimidazole (aebmz), Scheme 1. Novel structural features and reactivity patterns of these complexes present model character for VHPO. The catalytic potential of dioxovanadium(V) complexes as mimics for the sulfideperoxidase activity of

(3) Isupov, M. I.; Dalby, A. R.; Brindley, A. A.; Izumi, Y.; Tanabe, T.; Murshudov, G. N.; Littlechild, J. A. *J. Mol. Biol.* **2000**, *299*, 1035−1049.
(4) Messershmidt, A.; Wever, R. *Proc. Natl. Acad. Sci. U.S.A.* **1996**, *93*, 392−396.
(5) Butler, A. In *Bioinorgaic Catalysis*, 2nd ed.; Reedijk, J., Bouwman, E., Eds.; Marcel Dekker: New York, 1999; Chapter 5.
(6) (a) Smith, T. S., II; Pecoraro, V. L. *Inorg. Chem.* **2002**, *41*, 6754−6760. (b) Butler, A.; Clague, M. J.; Meister, G. E. *Chem. Rev.* **1994**, *94*, 625−638. (c) ten Brink, H. B.; Tuynman, A.; Dekker, H. L.; Hemrika, W.; Izumi, Y.; Oshiro, T.; Schoemaker, H. E.; Wever; R. *Inorg. Chem.* **1998**, *37*, 680−6784. (d) Andersson, M.; Willetts, A.; Allenmark, S. *J. Org. Chem.* **1997**, *62*, 845−8458. (e) Dembitsky, V. M. *Tetrahedron* **2003**, *59*, 4701−4720. (f) Rehder, D.; Santoni, G.; Licini, G. M.; Schulzke C.; Meier, B. *Coord. Chem. Rev.* **2003**, *237*, 53−63.
(7) (a) Ligtenbarg, A. G. J.; Hage, R.; Feringa, B. L. *Coord. Chem. Rev.* **2003**, 237, 89−101. (b) Conte, V.; Furia, F. Di.; Licini, G. *Appl. Catal., A* **1997**, *157*, 335−361.
(8) Xioping, L.; Kangjing, Z. *J. Crystallogr. Spectrosc. Res.* **1986**, *16*, 681.
(9) (a) Cornman, C. R.; Kampf, J.; Lah, M. S.; Pecoraro, V. L. *Inorg. Chem.* **1992**, *31*, 2035−2043. (b) Cornman C. R.; Colpas, G. J.; Hoeschele, J. D.; Kampf, J.; Pecoraro, V. L. *J. Am. Chem. Soc.* **1992**, *114*, 9925−9953. (c) Cornman, C. R.; Kampf, J.; Pecoraro, V. L. *Inorg. Chem.* **1992**, *31*, 1983−1985. (d) Smith, T. S., II; Root, C. A.; Kampf, J. W.; Rasmussen, P. G.; Pecoraro, V. L. *J. Am. Chem. Soc.* **2000**, *122*, 767−775.
(10) Fukui, K.; Ohya-Nishiguchi, H.; Kamada, H. *Inorg. Chem.* **1998**, *37*, 2326−2327.
(11) Vergopoulos, V.; Priebsch, W.; Fritzsche, M.; Rehder, D. *Inorg. Chem* **1993**, *32*, 1844−1849.
(12) Crans, D. C.; Keramidas, A. D.; Amin, S. S.; Anderson, O. P.; Miller, S. M. *J. Chem. Soc., Dalton Tans.* **1997**, 2799−2812.
(13) (a) Calviou, L. J.; Arber, J. M.; Collison, D.; Garner, C. D.; Clegg, W. *J. Chem. Soc., Chem. Commun.* **1992**, 654−656. (b) Keramidas, A. D.; Miller, S. M.; Anderson, O. P.; Crans, D. C. *J. Am. Chem. Soc.* **1997**, *119*, 8901−8915. (c) Crans, D. C.; Keramidas, A. D.; Hoover-Litty, H.; Anderson, O. P.; Miller, M. M.; Lemoine, L. M.; Pleasic-Williams, S.; Vandenberg, M.; Rossomando, A. J.; Sweet, L. J. *J. Am. Chem. Soc.* **1997**, *119*, 5447−5448. (d) Crans, D. C.; Schelble, S. M.; Theisen, L. A. *J. Org. Chem.* **1991**, *56*, 1266−1274. (e) Dutta, S. K.; Kumar, S. B.; Bhattacharyya, S.; Tiekink, E. R. T.; Chaudhury, M. *Inorg. Chem.*, **1997**, *36*, 4954−4958. (f) Dutta, S. K.; Samanta, S.; Kumar, S. B.; Han, O. H.; Burckel, P.; Pinkerton, A. A.; Chaudhury, M. *Inorg. Chem.* **1999**, *38*, 1982−1988. (g) Dutta, S. K., Samanta, S.; Mukhopadhyay, S.; Burckel, P.; Pinkerton, A. A.; Chaudhury, M. *Inorg. Chem.* **2002**, *41*, 2946−2952. (h) Samanta, S.; Ghosh, D.; Mukhopaqdhyay, S.; Endo, A.; Weakley, T. J. R.; Chaudhury, M. *Inorg. Chem.* **2003**, *42*, 1508−1517, also above paper of Rehder.
(14) (a) Maurya, M. R.; Khurana, S.; Schulzke C.; Rehder, D. *Eur. J. Inorg. Chem.* **2001**, 779−788. (b) Maurya, M. R.; Khurana, S.; Zhang, W.; Rehder, D. *Dalton Trans.* **2002**, 3015−3023. (c) Maurya, M. R.; Khurana, S.; Zhang, W.; Rehder, D. *Eur. J. Inorg. Chem.* **2002**, 1749−1760. (d) Maurya, M. R.; Khurana, S.; Shailendra, Azam, A.; Zhang, W.; Rehder, D. *Eur. J. Inorg. Chem.* **2003**, 1966−1973. (e) Maurya, M. R.; Agarwal, S.; Bader, C.; Rehder, D. *Eur. J. Inorg. Chem.* **2005**, 147−157. (f) Maurya, M. R.; Agarwal, S.; Bader, C.; Ebel, M.; Rehder, D. *Dalton Trans.* **2005**, 537−544. (g) Maurya, M. R.; Kumar, A.; Bhat, A. R.; Azam, A.; Bader, C.; Rehder, D. *Inorg. Chem.* **2006**, *45*, 1260−1269.

VHPO and for the oxidation of styrene by peroxide has also been studied.

Experimental Section

Materials. Glycine, β-alanine (Spectrochem, Mumbai, India), benzohydroxamic acid (Merck, Germany), *o*-phenylenediamine (phen), $VOSO_4 \cdot 5H_2O$, V_2O_5 (Loba Chemie, Mumbai, India), acetylacetone (Hacac, Aldrich, Milwaukee, WI), methyl phenyl sulfide (Alfa Aeaser, Ward Hill, MA), styrene (Acros Organics, Morris Plains, NJ), salicylaldehyde (sal), and 30% aqueous H_2O_2 (Qualigens, Mumbai, India) were used as obtained. $[VO(acac)_2]$,[15] 2-aminomethylbenzimidazole dihydrochloride (ambmz·2HCl),[12] and 2-aminoethylbenzimidazole dihydrochloride (aebmz·2HCl)[16] were prepared according to methods reported in the literature.

Instrumentation. Elemental analyses of the ligands and complexes were obtained from the Sophisticated Analytical Instrument Facility section of the Central Drug Research Institute, Lucknow, India. IR spectra were recorded as KBr pellets on a Nicolet NEXUS Aligent 1100 FT-IR spectrometer. UV−vis spectra were recorded in methanol or DMF with a Shimadzu UV-1601 PC UV−vis spectrophotometer. ^{1}H NMR spectra were recorded on a Bruker 200 MHz spectrometer, and ^{13}C and ^{51}V NMR spectra on a Bruker Avance 400 MHz spectrometer with the common parameter settings in DMSO-d_6. $\delta(^{51}V)$ values are quoted relative to $VOCl_3$ as external standard. EPR spectra were recorded with a Bruker ESP 300E spectrometer between 9.42 and 9.47 GHz, and EPR parameters were adjusted by simulation with the Bruker program system SimFonia. Thermograms of the complexes were recorded under oxygen atmosphere using a TG Stanton Redcroft STA 780 Instrument. Magnetic susceptibilities of oxovanadium(IV) complexes were determined at 298 K with a Vibrating Sample Magnetometer model 155, using nickel as a standard. Diamagnetic corrections were carried out with Pascal's increments.[17]

Crystal Structure Determinations. Data were collected on a Bruker SMART Apex CCD diffractometer at 153(2) K using a graphite monochromator and Mo K_α radiation ($\lambda = 0.71073$ Å). Hydrogen atoms were found or placed into calculated positions and included in the last cycles of refinement. Absorption corrections were carried out with SADABS. The program systems SHELXS 86 and SHELXL 93 were used throughout for the treatment and refinement of the data. CCDC numbers: **2**, 602598; **7**, 275152; **8**, 284222; **9**·$2H_2O$, 602599; **10**, 284221; **11**, 275153. Crystal data and details of the data collection and refinement for the new complexes are collected in Table 1.

Preparation of Ligands. (i) Hsal-ambmz (I). Ambmz·2HCl (1.10 g, 5 mmol) was dissolved in 15 mL of water and neutralized by adding aqueous K_2CO_3 solution (0.83 g, 6 mmol). A stirred solution of salicyaldehyde (0.61 g, 5 mmol) in 8 mL of methanol was added dropwise to the above solution with stirring within 1 h. During this period, yellow solid **I** slowly separated out. The solid was filtered off, washed thoroughly with water followed by petroleum ether, and dried in vacuo at room temperature. It was finally recrystallized from acetonitrile. Yield = 0.880 g (70%). Anal. Calcd for $C_{15}H_{13}N_3O$ (251.29): C, 71.70; H, 5.21; N, 16.72. Found: C, 70.89; H, 5.37; N, 16.52. Selected IR data (KBr, ν_{max}/cm^{-1}): 3430(OH), 2500−2700 (NH···O), 1636, 1617 (C═N). UV−vis [MeOH, λ_{max}/nm (ϵ/M^{-1} cm^{-1})]: 207(17 441), 256(8281), 274(7334), 281(6593), 324 (4065). ^{1}H NMR (DMSO-d_6, δ/ppm): 12.90(b, 1H, −OH), 8.95(s, 1H, −CH═N−); 6.98(d, 3H), 7.41(m, 4H), 7.67(d, 1H) (aromatic); 5.05(s, 2H, $-CH_2-$).

(ii) Hsal-aebmz (II). This ligand was synthesized by following the procedure outlined for **I**. Yield = 0.990 g (74%). Anal. Calcd for $C_{16}H_{15}N_3O$ (265.12): C, 72.43; H, 5.70; N, 15.84. Found: C, 71.88; H, 5.83; N, 15.73. Selected IR data (KBr, ν_{max}/cm^{-1}): 3400-(OH), 2500−2700 (NH···O), 1634 (C═N). UV−vis [MeOH, λ_{max}/nm (ϵ/M^{-1} cm^{-1})]: 208(25 760), 252(9404), 273(6240), 281(6278), 318(2239). ^{1}H NMR (DMSO-d_6, δ/ppm): 13.2(b, 1H, OH), 8.61-(s, 1H, −CH═N−); 6.80(t, 2H), 7.12(d, 2H), 7.31(t, 1H), 7.40(d, 1H), 7.50(d, 2H) (aromatic); 4.12(b, 4H, $-CH_2-$).

Preparation of Complexes. (i) [VO(acac)(sal-ambmz)] (1), [VO_2(acac-ambmz)] (2), and [VO(sal-phen)] (3). A stirred solution of Hsal-ambmz (1.26 g, 5 mmol) in dry methanol (10 mL) was treated with $[VO(acac)_2]$ (1.33 g, 5 mmol) dissolved in dry methanol (10 mL), and the resulting reaction mixture was refluxed for 2 h. Brown crystals of **1** along with some green solid separated out. After cooling to ambient temperature, the mixed solids were filtered off and thoroughly washed with CH_2Cl_2 (5 × 10 mL) to remove the green constituents and dried in a desiccator over silica gel. Yield = 0.98 g (47%). Anal. Calcd for $C_{20}H_{19}N_3O_4V$ (416.08): C, 57.68; H, 4.60; N, 10.10. Found: C, 56.93; H, 4.70; N, 9.86. Selected IR data (KBr, ν_{max}/cm^{-1}): 1632, 1600 (C═$N_{azomethine}$/N_{ring}), 920 (V═O). UV−vis [MeOH, λ_{max}/nm (ϵ/M^{-1} cm^{-1})]: 207(13 876), 239(10 609), 273(8617), 280(8141), 382-(1046), 554 (20). μ_{eff} (293 K) = 1.62 μ_B.

The filtrate and washings obtained from **1** were left open at ambient temperature for slow evaporation, as well as aerial oxidation, for ca. 2 days. During this period of time, green crystals separated out, which were collected by filtration and dried. Yield 35%. The major product obtained by this way was identified as **3** along with minor amount of **2**. **2** and **3** were separated by extracting **3** with CH_2Cl_2. Structures of both complexes were confirmed by single-crystal X-ray studies.

Alternate method for 2. A suspension of ambmz·2HCl (1.10 g, 5 mmol) in 10 mL of absolute ethanol was treated with anhydrous CH_3COONa (0.82 g, 10 mmol) with stirring. After 1 h, the white solid which had separated out was filtered off, and the filtrate was added to a solution of $[VO(acac)_2]$ (1.59 g, 6 mmol) dissolved in 10 mL of methanol. After 6 h of refluxing, the green solution was kept overnight at room temperature to yield green solid **2**. This was filtered off, washed with methanol, and dried. Green X-ray-quality crystals of **2** were obtained upon crystallization from dichloromethane. Yield = 0.855 g (55%). Anal. Calcd for $C_{13}H_{14}N_3O_3V$ (311.21): C, 50.17; H, 4.53; N, 13.50. Found: C, 50.11; H, 4.70; N, 13.33. Selected IR data (KBr, ν_{max}/cm^{-1}): 1627, 1598 (C═$N_{azomethine}$/N_{ring}), 958 (O═V═$O_{antisym}$), 888(O═V═O_{sym}). UV−vis [MeOH, λ_{max}/nm (ϵ/M^{-1} cm^{-1})]: 221(26 710), 271(8263), 279(8145), 323(4785). ^{51}V NMR (DMSO-d_6, δ/ppm): −558.1.

Alternate method for 3. To a stirred solution of Hsal-ambmz (1.26 g, 5 mmol) in 20 mL of methanol was added a hot solution of $VOSO_4$ (0.633 g, 2.5 mmol) dissolved in 40 mL of methanol, and the reaction mixture was refluxed for 1 h. After the solution was filtered, it was kept at room temperature for 2 days. Green solid **3** slowly separated out. This was filtered off, washed with methanol, and dried. To remove minor byproducts, the solid was taken up with CH_2Cl_2 and filtered. Evaporation of the filtrate to dryness gave pure **3**. Yield = 0.429 g, (45%).

This complex was also prepared by the reaction of $[VO(acac)_2]$ and H_2sal-phen in dry refluxing methanol. In a typical reaction, a solution of H_2sal-phen (1.58 g, 5 mmol) in 10 mL of dry methanol was added to a solution of $[VO(acac)_2]$ (1.59 g, 6 mmol) dissolved in 10 mL of the same solvent and the reaction mixture was refluxed

(15) Row: R. A.; Jones, M. M. *Inorg. Synth.* **1957**, *5*, 113−116.
(16) Ceson, L. A.; Day, A. R. *J. Org. Chem.* **1962**, *27*, 581−586.
(17) Dutta, R. L.; Syamal, A. *Elements of Magnetochemistry*, 2nd ed.; Affiliated East-West Press: New Delhi, 1993; p 8.

Table 1. Crystal Data and Structure Refinement Parameters

	2	**7**·$^1/_4H_2O$	**8**
empirical formula[a]	$C_{13}H_{14}N_3O_3V$	$C_{21}H_{21.5}N_3O_{4.25}V$	$C_{16}H_{14}N_3O_3V$
fw,[a] g mol^{-1}	311.21	435.36	347.24
cryst syst	monoclinic	triclinic	monoclinic
space group	*P*2(1)/*c*	$P\bar{1}$	*C*2/*c*
unit cell dimensions:			
a, Å	9.3698(10)	10.0544(17)	27.414(4)
α, deg		84.617(3)	
b, Å	10.5432(11)	14.279(2)	10.0644(16)
β, deg	103.519(2)	80.627(3)	109.626(3)
c, Å	13.5561(15)	15.354(3)	11.1461(18)
γ, deg		76.181(3)	
volume, Å^3	1302.1(2)	2108.4(6)	2896.6(8)
Z	2	4	8
calcd density, g cm^{-3}	1.588	1.371	1.593
absorption coefficient, mm^{-1}	0.772	0.503	0.704
F(000)	640	904	1424
crystal size, mm^3	0.60 × 0.22 × 0.07	0.4 × 0.1 × 0.1	0.26 × 0.24 × 0.14
θ range for data collection, deg	2.24−27.49	1.94−26.50	2.17−27.50
index ranges	$-11 \le h \le 11$	$-10 \le h \le 12$	$-21 \le h \le 35$
	$-13 \le k \le 12$	$-12 \le k \le 17$	$-12 \le k \le 13$
	$-17 \le l \le 16$	$-19 \le l \le 17$	$-14 \le l \le 12$
reflns collected	8353	12 726	9407
independent reflns	2885 [*R*(int) = 0.0321]	8412 [*R*(int) = 0.0348]	3261 [*R*(int) = 0.0523]
completeness to *θ* (max), %	96.5	96.1	97.9
data/restraints/params	2885/0/226	8412/2/543	3261/0/208
GOF on F^2	1.051	1.095	0.848
final *R* indices [$I > 2\sigma(I_0)$]	R1 = 0.0408,	R1 = 0.0825,	R1 = 0.0467,
	wR2 = 0.1069	wR2 = 0.2221	wR2 = 0.0846
R indices (all data)	R1 = 0.0447,	R1 = 0.1077,	R1 = 0.0771,
	*w*R2 = 0.1100	wR2 = 0.2347	wR2 = 0.0913
largest diff. peak/hole, eÅ^{-3}	0.599 and −0.316	1.244 and −0.835	0.567 and −0.534

	9	**10**	**11**
empirical formula[a]	$C_{32}H_{32}N_6O_{10}SV_2$	$C_{30}H_{20}N_6O_3V_2$	$C_{23}H_{19}N_4O_4V$
fw,[a] g mol^{-1}	794.58	614.40	466.36
cryst syst	monoclinic	triclinic	monoclinic
space group	*C*2/*c*	$P\bar{1}$	*P*21/*c*
unit cell dimensions:			
a, Å	17.5500(14)	9.850(5)	12.0354(5)
α, deg		80.374(9)	
b, Å	9.4055(7)	11.223(6)	18.7761(18)
β, deg	109.505(2)	83.382(9)	90.1990(10)
c, Å	21.3903(17)	13.558(7)	18.7346(8)
γ, deg		73.994(8)	
volume, Å^3	3328.2(4)	1416.5(13)	4233.6(3)
Z	4	2	8
calcd density, g cm^{-3}	1.586	1.440	1.463
absorption coefficient, mm^{-1}	0.693	0.702	0.507
F(000)	1632	624	1920
crystal size, mm^3	0.55 × 0.26 × 0.22	0.72 × 0.1 × 0.05	0.50 × 0.17 × 0.05
θ range for data collection, deg	2.46−27.00	1.53−28.01	1.69−27.50
index ranges	$-22 \le h \le 14$	$-12 \le h \le 12$	$-15 \le h \le 15$
	$-11 \le k \le 11$	$-14 \le k \le 14$	$-24 \le k \le 24$
	$-15 \le l \le 27$	$-17 \le l \le 17$	$-24 \le l \le 23$
reflns collected	10377	15696	50372
independent reflns	3594 [*R*(int) = 0.0320]	6332 [*R*(int) = 0.1508]	9675 [*R*(int) = 0.0692]
completeness to *θ* (max), %	98.9	28.01	99.5
data/restraints/params	3594/3/237	6332/0/384	9675/0 /577
GOF on F^2	1.026	0.901	0.830
final *R* indices [$I > 2\sigma(I_0)$]	R1 = 0.0421,	R1 = 0.0809,	R1 = 0.0431,
	wR2 = 0.1139	wR2 = 0.1681	wR2 = 0.0717
R indices (all data)	R1 = 0.0541,	R1 = 0.1653,	R1 = 0.0818,
	wR2 = 0.1188	wR2 = 0.2142	wR2 = 0.0785
largest diff. peak/hole, eÅ^{-3}	0.865 and −0.338	0.933 and −0.708	0.708 and −0.441
		92.8%	

[a] Per formula unit.

for 1 h. Keeping the green solution thus obtained for 2 days resulted in the separation of green crystalline solid **3**. This was filtered off, washed with methanol, and dried in vacuo. Yield = 1.105 g (55%). Anal. Calcd for $C_{20}H_{14}N_2O_3V$ (381.28): C, 63.0; H, 3.70; N, 7.55. Found: C, 63.13; H, 3.83; N, 7.34. μ_{eff} (293 K) = 1.75 μ_B. IR data (KBr, ν_{max}/cm^{-1}): 1606, 1579 (C═$N_{azomethine}$), 986 (V═O).

(ii) [VO_2(sal-ambmz)] (4). Method A. Compound **1** (2.08 g, 5 mmol) was suspended in methanol (200 mL), and air was slowly passed through the suspension for ca. 3 days with occasional shaking. During this time, the brown suspension slowly disappeared, and light yellow solid **4** separated out. This was filtered off, washed with hot methanol, and dried at ambient temperature. Finally, it

was purified by recrystallization from hot methanol. Yield = 1.67 g (80%). Anal. Calcd for $C_{15}H_{12}N_3O_3V$ (333.22): C, 54.07; H, 3.63; N, 12.61. Found: C, 53.76; H, 3.76; N, 12.42. Selected IR data (KBr, ν_{max}/cm^{-1}): 1624, 1599 (C═$N_{azomethine}$/N_{ring}), 940 (O═V═$O_{antisym}$), 908(O═V═O_{sym}). UV−vis (MeOH, λ_{max}/nm): 210, 237, 273, 280, 388. ^{1}H NMR (DMSO-d_6, δ/ppm): 9.10(s, 1H, −CH═N−); 6.86(d, 3H), 7.38(s, 1H), 7.50(t, 1H), 7.60(d, 1H), 7.66(d, 1H), 8.10(d, 1H) (aromatic); 5.52(s, 2H, $-CH_2$-). ^{51}V NMR (DMSO-d_6, δ/ppm): −567.8.

Method B. A solution of [VO(acac)$_2$] (1.33 g, 5 mmol) in methanol (50 mL) was stirred overnight in air, where the solution slowly changed to orange-red. A solution of Hsal-ambmz (1.03 g, 5 mmol) in methanol (10 mL) was added, and the reaction mixture was stirred at ambient temperature for 6 h. The light yellow solid that precipitated slowly during this period of time was filtered off, washed with methanol, and dried. Yield = 0.866 g (52%). IR and electronic spectroscopic data matched well with **4** prepared according to method A.

(iii) [{VO(sal-ambmz)}$_2$SO$_4$] (5). A methanolic solution of $VOSO_4 \cdot 5H_2O$ (0.506 g, 2 mmol in 40 mL) was stirred with Hsal-ambmz (1.0 g, 4 mmol) dissolved in 15 mL of methanol at room temperature for 6 h. Thereafter, the reaction mixture was kept overnight at room temperature. A blue precipitate was filtered off, washed with methanol, and dried. Yield = 0.31 g (37%). Anal. Calcd for $C_{30}H_{24}N_6O_8SV_2$ (766.53): C, 49.28; H, 3.29; N, 11.49. Found: C, 48.73; H, 3.01; N, 11.37. Selected IR data (KBr, ν_{max}/cm^{-1}): 1630, 1594(C═$N_{azomethine}$/N_{ring}), 970 (V═O). UV−vis (MeOH, λ_{max}/nm): 211, 238, 273, 281, 391. μ_{eff} (293 K) = 1.53 μ_B.

The filtrate was allowed to slowly evaporate at room temperature. A green solid which had formed within 24 h was filtered off and washed with methanol. After recrystallization from CH_2Cl_2, it was identified as **3**. Yield = 0.37 g (48%).

(iv) [VO(bha)(sal-ambmz)] (6). A stirred solution of **1** (0.832 g, 2 mmol) in hot methanol (60 mL) was treated with benzohydroxamic acid (0.274 g, 2 mmol), and the reaction mixture was refluxed on a water bath for 4 h. After the volume of the solvent was reduced to ca. 20 mL and the mixture was cooled to room temperature, blackish **6** separated out overnight. This was filtered off, washed with methanol, and dried in vacuo. Yield = 0.38 g (42%); Anal. Calcd for $C_{22}H_{17}N_4O_4V$ (452.34): C, 58.42; H, 3.79; N, 12.39. Found: C, 57.89; H, 4.05; N, 12.02. Selected IR data (KBr, ν_{max}/cm^{-1}): 1654, 1604 (C═$N_{azomethine}$/N_{ring}), 970 (V═O). UV−vis [MeOH, λ_{max}/nm (ϵ/M^{-1} cm^{-1})]: 210 (17 885), 220 (16 750), 282 (7373), 382 (1860), 600 (435). ^{1}H NMR (DMSO-d_6, δ/ppm): 8.67(s, 1H, −CH═N−); 6.60(d, 1H), 6.76(t, 1H), 7.40-(m, 5H), 7.49(q, 2H), 7.63(d, 2H), 8.41(d, 2H) (aromatic); 4.37(t, 2H), 4.16(t, 2H)($-CH_2-$).

(v) [VO(acac)(sal-aebmz)](7). A stirred solution of Hsal-aebmz (1.33 g, 5 mmol) in dry methanol (10 mL) was treated with a methanolic solution of [VO(acac)$_2$] (1.33 g, 5 mmol). The resulting reaction mixture was refluxed on a water bath for 2 h. After the mixture cooled to room temperature, a brown crystalline solid of **7** was obtained, which was filtered off, washed with methanol, and dried in vacuo. Yield = 1.35 g (63%); Anal. Calcd for $C_{21}H_{21}N_3O_4V$ (430.36): C, 58.61; H, 4.92; N, 9.76. Found: C, 58.66; H, 5.10; N, 9.55. Selected IR data (KBr, ν_{max}/cm^{-1}): 1630, 1597 (C═$N_{azomethine}$/N_{ring}), 950 (V═O). UV−vis [MeOH, λ_{max}/nm (ϵ/M^{-1} cm^{-1})]: 208(18 669), 239(10 647), 273(8600), 279(8165), 322-(1532), 382(1046), 540(35), 700(225). μ_{eff} (293 K) = 0.59 μ_B.

(vi) [VO$_2$(sal-aebmz)] (8). Complex **8** was prepared from **7**, using the method mentioned for **4**, replacing Hsal-ambmz for Hsal-aebmz. Yield = 1.47 g (85%). Anal. Calcd for $C_{16}H_{14}N_3O_3V$ (347.3): C, 55.34; H, 4.06; N, 12.10. Found: C, 54.94; H, 3.98; N, 12.26. Selected IR data (KBr, ν_{max}/cm^{-1}): 1624 (C═$N_{azomethine}$/N_{ring}), 948 (O═V═$O_{antisym}$), 917(O═V═O_{sym}). UV−vis [MeOH, λ_{max}/nm (ϵ/M^{-1} cm^{-1})]: 212(24 092), 252(13 494), 273(9127), 281-(8726), 313(3152), 405(452). ^{1}H NMR (DMSO-d_6, δ/ppm): 8.87-(s, 1H, −CH═N−); 6.80(t, 2H), 7.12(s, 1H), 7.43(d, 2H), 7.54(t, 2H), 8.92(d, 1H) (aromatic); 4.17(b, 4H, $-CH_2-$). ^{51}V NMR (DMSO-d_6, δ/ppm): −540.3. Complex **8** was also prepared following the method B outlined for **4**.

(vii) [{VO(sal-aebmz)}$_2$SO$_4$]·2H$_2$O (9). A methanolic solution of $VOSO_4 \cdot 5H_2O$ (0.506 g, 2 mmol in 40 mL) was added to a solution of Hsal-aebmz (1.060 g, 4 mmol) dissolved in 20 mL of methanol, and the resulting reaction mixture was refluxed for 1 h. After being kept at room temperature for ca. 12 h, the solution was filtered to give a cream-colored solid and a brown filtrate with a touch of blue. The filtrate was kept for 24 h, during which time blue solid **9** separated out. This was removed by filtration, and the filtrate was kept safely. The blue solid was washed with water, followed by methanol, and dried. Yield = 0.30 g (30%). Anal. Calcd for $C_{32}H_{32}N_6O_{10}SV_2$ (794.58): C, 48.37; H, 4.06; N, 10.58. Found: C, 48.56; H, 3.93; N, 10.64. IR data (KBr, ν_{max}/cm^{-1}): 1627, 1573(C═$N_{azomethine}$/N_{ring}), 968 (V═O). UV−vis (MeOH, λ_{max}/nm): 242, 273, 281, 325. μ_{eff} (293 K) = 1.69 μ_B. The original reaction mixture (before workup for the recovery of **9**) was allowed to stand for a couple of days to give a heterogeneous mixtures of crystals of blue **9** and light-yellow **8**, both suitable for X-ray structural analyses.

(viii) [VO(sal-aebmz)$_2$] (10). Keeping the filtrate from the above reaction (i.e., after removing **9**) for ca. 24 h gave a light-yellow solid along with contamination of a green solid. The solids were separated by filtration, and the brown filtrate was kept at room temperature overnight to afford brown solid **10**, which was filtered off, washed with water followed by methanol, and dried. X-ray-quality crystals of **10** were obtained by recrystallization from methanol. Yield = 1.43 g (63%). Anal. Calcd for $C_{32}H_{28}N_6O_3V$ (595.55): C, 64.54; H, 4.74; N, 14.11. Found: C, 64.51; H, 4.80; N, 14.02. Selected IR data (KBr, ν_{max}/cm^{-1}): 1643, 1625 (C═$N_{azomethine}$/N_{ring}), 970 (V═O). UV−vis [MeOH, λ_{max}/nm (ϵ/M^{-1} cm^{-1})]: 207 (13 894), 241(8052), 274 (4844), 279 (4677), 318 (1450), 378 (1079), 532 (132), 754 (30). μ_{eff} (293 K) = 1.78 μ_B.

The co-mixture of light yellow and green solid was thoroughly washed with CH_2Cl_2 and dried. The complex obtained in 23% yield was identified as **8**. On evaporating the filtrate, green complex **3** was obtained just in sufficient amounts to establish its identity by IR and electronic spectra.

(ix) [VO(bha)(sal-aebmz)] (11). Complex **11** was prepared following the procedure outlined for **6**. After the volume of the solvent was reduced to ca. 20 mL and the mixture was cooled to room temperature, blackish crystals of **11** slowly separated out within 2 days. This was filtered off, washed with methanol, and dried in vacuo. Yield = 1.43 g (63%). Anal. Calcd for $C_{23}H_{19}N_4O_4V$ (466.37): C, 59.23; H, 4.11; N, 12.01. Found: C, 59.26; H, 3.79; N, 11.53. Selected IR data (KBr, ν_{max}/cm^{-1}): 1640, 1611 (C═$N_{azomethine}$/N_{ring}), 967 (V═O). UV−vis [MeOH, λ_{max}/nm (ϵ/M^{-1} cm^{-1})]: 215(25 587), 223(25 623), 251(17 850), 274(13 823), 282-(13 832), 318(5547), 390(1431), 480(422), 643(674). ^{1}H NMR (DMSO-d_6, δ/ppm): 8.87(s, 1H, −CH═N−); 6.73(d, 1H), 6.84(t, 1H), 7.54(t,1H),7.45(m, 5H), 7.55(q, 2H), 7.73(d, 2H), 8.36(d, 1H) (aromatic); 4.12(t, 2H), 4.34(t, 2H)($-CH_2-$). ^{51}V NMR (DMSO-d_6, δ/ppm): 71.2 and −542.3 (very weak signal corresponding to **6**).

(x) [VO(O$_2$)(sal-aebmz)] (12). Complex **7** (0.430 g, 1 mmol) was dissolved in hot methanol (60 mL). This solution was cooled

to ca. 10 °C and treated, under stirring, dropwise within 15 min with a solution of aqueous 30% H_2O_2 (0.5 mL) in 5 mL of methanol. A cream solid slowly separated. After 30 min, this was filtered off, washed with cold methanol, and dried in vacuo. Yield = 0.29 g (80%). An elemental analysis of the complex could not be obtained due to its decomposition at room temperature. Selected IR data (KBr, ν_{max}/cm^{-1}): 1625 ($C{=}N_{azomethine}/N_{ring}$), 965 (V=O). 878 (O−O), 755 [$V(O_2)_{antisym}$], 614 [$V(O_2)_{sym}$]. UV−vis (MeOH, λ_{max}/nm): 212, 256, 269, 276, 279, 321, 405.

Catalytic Reactions. (i) Oxidation of Methyl Phenyl Sulfide. The oxidation of methyl phenyl sulfide was achieved with the complexes **2**, **4**, and **8** as catalysts. The reaction was carried out at ambient temperature in a 50 mL flask equipped with a magnetic stirrer. In a typical reaction, methyl phenyl sulfide (0.62 g, 5 mmol) was dissolved in 20 mL of acetonitrile. After addition of aqueous 30% H_2O_2 (0.57 g, 5 mmol) and catalyst (15 mg), the reaction mixture was stirred for 3 h. During this period of time, the formation of reaction products was monitored by GC, withdrawing small aliquots from the reaction mixture after specific intervals of time and confirming the identity of the products by GC-MS.

(ii) Oxidation of Styrene. Complexes **2**, **4**, and **8** were also tested as catalysts in the oxidation of styrene. Styrene (0.51 g, 5 mmol) and aqueous 30% H_2O_2 (0.57 g, 5 mmol) were taken in 25 mL of acetonitrile, and the reaction mixture was heated to 80 °C in an oil bath while stirring. Catalyst (20 mg) was added to the reaction mixture. The formation of the oxidation products was monitored by GC, and the identity of the products analyzed as noted above. To find out the effect of H_2O_2 on the oxidation of styrene, its concentration was varied while keeping the other conditions constant.

Results and Discussion

Synthesis, Reactivity, and Solid-State Characteristics. Chart 1 provides an overview of the complexes described in this contribution. Structures of these complexes are based on spectroscopic (IR, UV−vis, EPR, ^1H, ^{13}C, and ^{51}V NMR) data, elemental analyses, and X-ray diffraction analyses of complexes **2**, **3**, **7**, **8**, **9**, **10**, and **11**.

Reaction between equimolar amounts of [$VO(acac)_2$] and the ligands **I** or **II** (cf. Scheme 1) in dry, refluxing methanol yields the brown oxovanadium(IV) complexes **1** or **2**, respectively. The formation of **1** and **2** is accompanied by a complex reaction pattern depicted for **I** in Scheme 2: Keeping the filtrate obtained after separating **1** exposed to air, resulted in the formation of **2** and the known complex **3**. Apparently, while part of Hsal-ambmz reacted with [$VO(acac)_2$] to give **1** (reaction step 1 in Scheme 2), Hsal-ambmz was concomitantly split hydrolytically (step 2) to give 2-aminomethylbenzimidazole (ambmz) and salicylaldehyde (Hsal). Part of the ambmz thus produced reacted with [$VO(acac)_2$], accompanied by aerial oxidation, to give **2** (step 3), while the remaining part further decomposed to *o*-phenylenediamine (step 4). The *o*-phenylenediamine, forming the Schiff base H_2sal-phen with salicylaldehyde (step 5), further reacts with [$VO(acac)_2$] to yield **3** (step 6). The nature of the second product of decomposition of ambmz in step 4 is not clear. In crystals of **3**, dimethylformamide co-crystallizes, suggesting intermediate formation of amino-acetaldehyde, followed by rearrangement of the N−C skeleton. Complex **2** can also be prepared directly by reacting [$VO(acac)_2$] with aebmz followed by aerial oxidation.

Chart 1

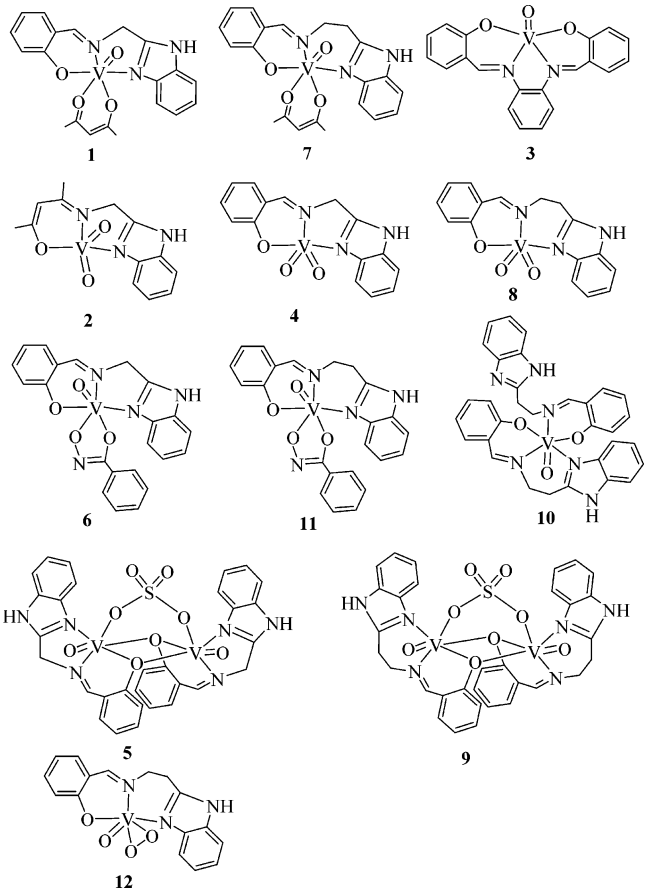

Scheme 2

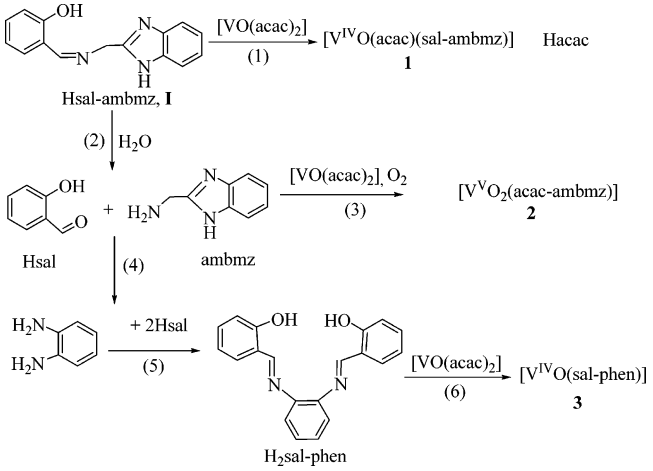

On aerial oxidation of **1** in methanol, the dioxovanadium(V) complex **4** was obtained (eq 3). Similarly, complex **7** can be oxidized in methanol to **8**. Further, **4** and **8** were obtained from the reaction of aerially oxidized solutions of [$VO(acac)_2$] with **I** and **II**, respectively, in methanol.

$$2[\underset{\mathbf{1}}{VO^{IV}(acac)(sal\text{-}ambmz)}] + {}^1/_2O_2 + H_2O \rightarrow \underset{\mathbf{4}}{2[VO_2(sal\text{-}ambmz)]} + 2Hacac \quad (3)$$

Reaction of $VOSO_4 \cdot 5H_2O$ with these ligands in the ratio 1:2 (metal/ligand) provided a series of complexes. Ligand

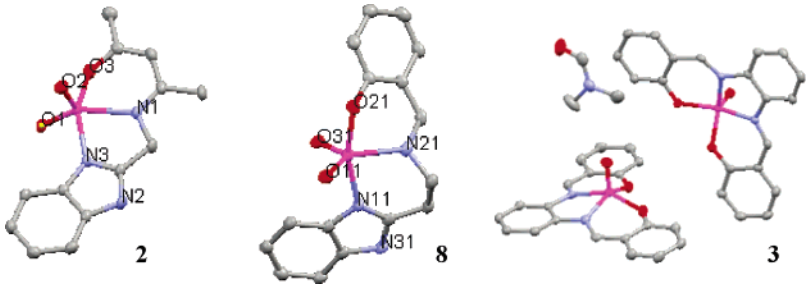

Figure 2. Structure representations of complexes **2**, **3**, and **8**. Red, O; magenta, V; blue, N.

Table 2. Selected Bond Lengths (Å) and Angles (deg) for **2**, **7** (Only One of the Two Molecules in the Asymmetric Unit), **8**, and **10**

	2	**8**	**7**	**10**
		bond lengths (Å)		
V=O	V−O2 1.6104(16)	V−O31 1.6276(18)	V1−O11 1.601(4)	V−O11 1.594(3)
V=O	V−O1 1.6732(16)	V−O11 1.6089(19)		
phenolate−O	V−O3 1.9266(16)	V−O21 1.9300(19)	V1−O21 1.981(4)	V−O21/O22 1.966(4)/2.054(4)
azomethine−N	V−N1 2.1588(17)	V−N21 2.114(2)	V1−N21 2.068(5)	V−N21/N22 2.1124(4)/2.124(4)
imidazole−N	V−N3 2.0653(17)	V−N11 2.121(2)	V1−N11 2.133(5)	V−N11 2.103(4)
			V1−O31 1.995(4)	
			V1−O41 2.158(4)	
		bond angles (deg)		
	O2−V−N1 107.58(7)	O11−V−N21 127.45(10)	O11−V1−O41 173.52(18)	O11−V−O22 173.82(17)
	O3−V−N3 150.48(7)	O21−V−N11 s163.20(9)	O11−V1−N11 94.32(19)	O21−V−N11 166.54(15)
	O3−V−N1 83.10(7)	O21−V−N21 81.79(9)	N11−V1−N21 88.62(18)	O11−V−N11 92.91(17)
	N1−V−N3 75.48(7)	N21−V−N1 81.45(9)	N21−V1−O21 87.13(17)	O21−V−N21 87.35(16)
	O1−V−O2 107.82(8)	O11−V−O31 110.29(10)	O21−V1−N11 162.93(17)	O22−V−N22 82.14(15)
				N11−V−N21 87.90(17)

II, e.g., gave **9**, **10**, **8** (eqs 4−6), and **3** along with $[H_2$sal-aebmz$]^+[HSO_4]^-$ in small amount. These complexes can be separated one by one from the reaction mixture and crystallized with suitable solvents. Similarly, ligand **I**, when reacted with $VOSO_4$ in methanol at room temperature gave **5** as the major product, while heating of the reaction mixture yielded a mixture of **3** and the dinuclear complex **5**. From the filtrate, small amounts of cream-colored and brown solids were also isolated which are likely to be $[VO_2$(sal-ambmz)] and [VO-(sal-ambmz)$_2$], respectively.

$$2VOSO_4 + 2\text{Hsal-aebmz} \xrightarrow[\textbf{II}]{} [\{VO(\mu\text{-sal-aebmz})\}_2\mu\text{-}SO_4] + H_2SO_4 \quad (4)$$
$$\textbf{9}$$

$$VOSO_4 + 2\text{Hsal-aebmz} \xrightarrow[\textbf{II}]{} [VO(\eta^2\text{-sal-aebmz})\,(\eta^3\text{-sal-aebmz})] + H_2SO_4 \quad (5)$$
$$\textbf{10}$$

$$2VOSO_4 + 2\text{Hsal-aebmz} + {}^1/_2O_2 + H_2O \xrightarrow[\textbf{II}]{} 2[VO_2(\text{sal-aebmz})] + 2H_2SO_4 \quad (6)$$
$$\textbf{8}$$

Treatment of **1** and **7** with benzohydroxamic acid in methanol under aerobic conditions resulted in the formation of the mixed-ligand complexes **6** and **11**, as represented by eq 7.

$$2[VO(acac)(L)] + 2H_2bha + {}^1/_2O_2 + 2H^+ \rightarrow 2[VO(bha)(L)] + 2Hacac + H_2O \quad (7)$$
$$\text{HL} = \textbf{I}, \textbf{6}; \text{HL} = \textbf{II}, \textbf{11}'$$

Complexes **4**, **5**, and **9** are soluble in DMSO and DMF only; others also dissolve in methanol, while **3** is soluble in CH_2Cl_2. Complexes **1** and **7** exhibit a magnetic moment of 1.62 and 0.59 μ_B, respectively. The comparatively low value for **1** and the very low value for **7** are due to partial oxidation to the dioxo species. Complex **7** is, in fact, sufficiently more susceptible to aerial oxidation than **1**. Complexes **5** and **9** exhibit subnormal magnetic moment value of 1.53 and 1.69 μ_B, respectively, possibly due to magnetic exchange interaction between two vanadium(IV) centers through bridging phenolato and sulfato groups. Other complexes, e.g., **3** and **10**, exhibit normal magnetic moment values of 1.75 and 1.78 μ_B.

Structure Descriptions. The dioxo complexes **2** and **8** are depicted in Figure 2, bonding parameters in Table 2. The two complexes represent distorted trigonal bipyramids; the τ values are 0.71 for **2** and 0.60 for **8** ($\tau = 1$ for an ideal trigonal bipyramid, $\tau = 0$ for an ideal square pyramid). The phenolate O (O3 and O21, respectively) and the imidazole N (N3 and N11) are in the axial positions. The arrangement of the O_4N donor sets in these two dioxovanadium(V) complexes, in particular in **2**, thus compares with the active site in VHPO (Figure 1). In the crystalline assembly, **2** forms one-dimensional chains via hydrogen-bonding contacts between one of the doubly bonded oxo groups and the imidazole NH, d(O1−N2) = 2.754 Å. Consequently, the d(V−O1) = 1.673 Å is clearly longer than d(V−O2) = 1.610 Å, and "normal" V=O bonds in other oxovanadium complexes, commonly ranging from 1.57 to 1.62 Å.[1e,18−20]

The known[21] oxovanadium(IV) complex **3**, also shown in Figure 3, is an ideal square-planar complex. One molecule

(18) Santoni, G.; Rehder, D. *J. Inorg. Biochem.* **2004**, *98*, 758−764.

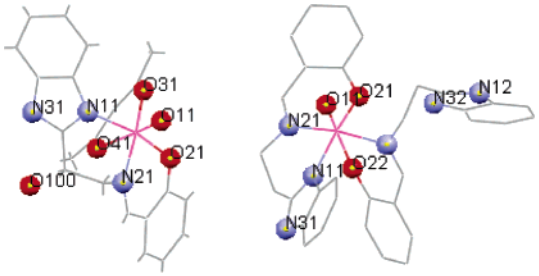

Figure 3. Structures of **7** (left) and **10** (right). For **7**, only one of the two independent molecules in the asymmetric unit is shown. O100 represents a water molecule with an occupancy of 25%.

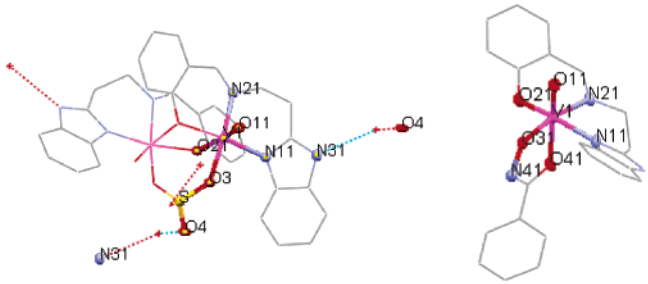

Figure 4. Structures of **9**·2H_2O (left), including hydrogen bonds (dashed lines) and the *C* enantiomer of **11** (right).

of dimethylformamide co-crystallizes with two molecules of **3**, the closest contact, 3.217 Å, being that between the axial oxo group and one of the methyl carbons. The origin of the DMF is unclear; it may arise from the decomposition of 2-aminomethylbenzimidazole; cf. step 4 in Scheme 2.

The oxovanadium(IV) complexes containing the Schiff base sal-aebmz (**7** and **10**) are shown, with the octahedrally coordinated vanadium moiety high-lighted, in Figure 3. Bonding parameters are contained in Table 2. One of the ligands in **10 c**oordinates in the tridentate mode, the other one in the bidentate mode, leaving the benzimidazole moiety dangling. The axis of the octahedron is defined by the doubly bonded oxygen and the phenolate O (O22) of the bidentate ligand. The corresponding ligand functions in **7** are the oxo group and the acac oxygen, O41. Vanadium is displaced (toward the axial oxo group) from the plane spanned by the four equatorial ligands by 0.276 (**7**) and 0.226 Å (**10**). Bonding parameters are in the usual range; the bond lengths to the functions trans to the oxo group, O41 and O22, respectively, are somewhat elongated as a consequence of the trans influence.

The asymmetric unit of **7** contains two independent molecules in hydrogen-bonding contact via the imidazole NH and the phenolate O; *d*(O21···N32) = 2.793 Å and *d*(O22···N31) = 2.742 Å. Two waters of crystallization, each with an occupancy of 25%, are involved in H-bonding contacts (2.886 Å) to oxo functions of the acac co-ligand. There is an intramolecular hydrogen bond in **10**, linking the phenolate O21 of the tridentate ligand to N32 of the dangling part of the bidentate ligand; *d*(O21···HN32) = 2.794 Å. In addition, intermolecular hydrogen bonds between N12 and N31, *d*(N12···HN31) = 2.803 Å, give rise to infinite chains.

In the dinuclear complex **9** (Figure 4 left, and Table 3), with the two halves of the molecule related by a 2-fold axis, the two V=O groups, bridged by the sulfate-oxygens O3 and O3′ and the phenolate-oxygens O21 and O21′, are oriented anti-coplanar.[22] The distance of V from the plane spanned by O3, O21, N11, and N21 amounts to 0.263 Å. Two waters of crystallization (O5) interlink the molecules in the crystal lattice by forming hydrogen bonds to the sulfate O4 (*d*(O5···O4) = 2.803 Å) and to the imidazole N31 (*d*(O5···HN31) = 2.803 Å).

Complex **11** (Figure 4, right), which contains a hydroxamato ligand along with sal-aebmz, crystallizes in the centrosymmetric space group *P*21/*c*. There are two molecules in the asymmetric unit, with the asymmetric vanadium center in the *A* and the *C* configuration, respectively. The oxo group O11 and the benzohydroxamate oxygen O41 are in the axis. The remaining functions form a plane, from which V1 (the center of the *C* enantiomer) is displaced by 0.2553 Å. The corresponding displacement of V2 in the *A* enantiomer is 0.2833 Å. The geometry of the coordination sphere, a distorted octahedron, and the bonding parameters compare to those of other hydroxamato-oxovanadium complexes with hydroxamate in a mixed-ligand coordination sphere.[23,24]

TGA Studies. All complexes were dried at ca. 120 °C before running their thermograms under oxygen atmosphere. The TGA profiles of complexes **1**, **7**, and **11**, i.e., the complexes with the co-ligands acac or bha, show three overlapping decomposition steps. The first weight loss starts at ca. 220 (**1** and **7**) or 190 °C (**11**) and is completed at ca. 395 °C. On comparing these decomposition patterns with those of the dioxo analogues **2**, **4**, and **8**, it is clear that decomposition involves the co-ligand. However, the observed values always are less than the calculated ones. The two following decomposition steps, completed at ca. 500 °C, are not clearly distinct. The total mass loss, including the first step, corresponds to the value calculated for the loss of the entire organic moieties. The remaining residues correspond to the formation of V_2O_5 as the final product (found/calcd: **1**, 22.0/21.9%; **7**, 20.5/21.1%; **9**, 18.4/19.5%). The dioxovanadium(V) complex **4** decomposes in a single step in the narrow temperature range 260−320 °C, while **8** decomposes in two overlapping steps in the 260−470 °C range, again yielding V_2O_5 as the final product.

IR Spectral Studies. The oxovanadium(IV) complexes **1**, **5**, **7**, **9**, and **10** and the oxovanadium(V) complexes **6** and **11** display one sharp band in the 920−970 cm^{-1} region due to the ν(V=O) mode. There are two such bands between 888 and 958 cm^{-1} in the dioxovanadium(V) complexes **2**, **4**, and **8**, corresponding to the $\nu_{antisym}$(O=V=O) and ν_{sym}-(O=V=O) modes. The peroxo complex **12** shows three IR active vibration modes associated with the peroxo moiety

(19) Cornman, C. R.; Geiser-Bush, K. M.; Rowley, S. P.; Boyle, P. D. *Inorg. Chem.* **1997**, *36*, 6401−6408.
(20) Mahroof-Tahir, M.; Keramidas, A. D.; Goldfarb, R. B.; Anderson, O. P.; Miller, M. M.; Crans, D. C. *Inorg. Chem.* **1997**, *36*, 1657−16668.
(21) Wang, X.; Zhang, X. M.; Liu, H. X. *Polyhedron* **1995**, *13*, 293−296.
(22) Plass, W. *Angew. Chem., Int. Ed.* **1996**, *33*, 627−631.
(23) Cornman, C.R.; Colpas, G. J.; Hoeschele, J. D.; Kampf, J.; Pecoraro, V. L. *J. Am. Chem. Soc.* **1992**, *114*, 9925−9933.
(24) Gao, S.; Weng, Z.-Q.; Liu, S.-X. *Polyhedron* **1998**, *17*, 3595−3606.

Table 3. Selected Bond Lengths (Å) and Angles (deg) for **9** and **11** (*C* Isomer Only)

9		**11**	
bond lengths (Å)	bond angles (deg)	bond lengths (Å)	bond angles (deg)
V−O11 1.5891(18)	O11−V−O21′ 174.15(8)	V1−O11 1.5898(15)	O11−V1−O41 170.15(7)
V−O3 1.9893(16	O3−V−N21 167.46(7)	V1−O41 2.1274(16)	O31−V1−N21 95.79
V−O21 1.9826(17)	O21−V−N11 162.69(8)	V1−O31 1.8440(15)	O21−V1−N11 163.17(7)
V−O21′ 2.2506(17)	O21−V−N21 87.20(7)	V1−O21 1.8995(15)	O31−V1−O41 76.33(6)
V−N11 2.115(2)	N11−V−N21 90.16(7)	V1−N11 2.0901(18)	O21−V1−N21 84.14(7)
V−N21 2.1039(19)		V1−N21 2.1514(18)	N11−V1−N21 84.40(7)

Table 4. EPR Parameters[a] of DMSO Solutions of Complexes **1**, **7**, and **9**

	g_{iso}	A_{iso}	g_{xy}	g_z	A_{xy}	A_z	A_z(calcd)
1	1.985	90	1.98	1.945	60	165	169
7	1.985	90	1.98	1.95	60	166	169
9	1.985	90	1.98	1.945	60	168	169

[a] Units for *A*: 10^{-4} cm^{-1}.

$\{V(O_2)^{3+}\}$ at 878, 755, and 614 cm^{-1}, and these are assigned to the O−O intra-stretch (ν_1), the antisymmetric $V(O_2)$ stretch (ν_3), and the symmetric $V(O_2)$ stretch (ν_2), respectively. The presence of these bands confirms the common η^2-coordination of the peroxo group. In addition, these complexes exhibit an intense ν(V═O) stretch at 965 cm^{-1}.[25]

IR spectra of the ligands **I** and **II** exhibit one or two sharp bands between 1615 and 1636 cm^{-1} due to ν(C═N) (azomethine/ring stretch). These bands move toward lower wavenumbers on coordination, indicating coordination of the azomethine/ring nitrogen to the vanadium. The presence of several medium intensity bands between 2500 and 2700 cm^{-1} in the ligands, as well as in most of the complexes, hints toward the existence of hydrogen bonding between NH of benzimidazole and other electronegative atoms. In addition, complexes **5** and **9** exhibit two bands (1125 and 1050 cm^{-1} in **5**; 1130 and 1034 cm^{-1} in **9**) in the ν_3 and one band (613 cm^{-1} in **5** and 606 cm^{-1} in **9**) in the ν_4 regions of the sulfate group, and these are well within the range reported for complexes bridged by the bidentate sulfato ligand. [26]

EPR Studies. EPR parameters have been obtained for the complexes **1**, **7**, and **9**. The isotropic and anisotropic parameters are listed in Table 4. The anisotropic spectra are axial. Also listed in Table 4 are calculated parallel hyperfine coupling constants, A_z. The calculations were carried out according to the additivity rule, employing recent listings of the partial contributions of the equatorial ligand functions.[27] The following partial contributions were used. Phenolate 38.9,[27] acac 43.5,[28] imino N 41.6,[27b] and imidazole N 45 × 10^{-4} cm^{-1}.[9d] The contribution of imidazole, depending on its orientation with respect to the V═O bond, ranges from 40 (parallel) to 45 × 10^{-4} cm^{-1} (perpendicular).[9d,29] In our complexes, the dihedral angles are 94.32° and 93.93° for **7** (and we presuppose that the situation is comparable for **1**) and 97.88° for **9**. For sulfate O, the contribution of which to A_z does not seem to have been reported, we have employed a value of 44 × 10^{-4} cm^{-1}, assuming a coordinating strength between water and carboxylate. Within the limits of error, the experimental A_z agree with the calculated ones, suggesting that the solution structure at low temperature does not significantly deviate from the structure in the crystalline solid state.

Electronic Spectral Studies. Electronic absorption spectral data of the ligands and complexes are given in the Experimental Section. The UV spectra of the ligands show five sharp absorption maxima. The most probable assignment of the first two bands is $\varphi \rightarrow \varphi^*$ and $\pi \rightarrow \pi^*$, while the last band is assignable to the n $\rightarrow \pi^*$ transition. Assignment of other intraligand bands was not possible. A weak shoulder due to hydrogen bonding appears along with these bands. On complexation, the $\varphi \rightarrow \varphi^*$ and $\pi \rightarrow \pi^*$ transitions shift toward higher wavelengths while the n $\rightarrow \pi^*$ transition merges with an additional broad band due to the ligand-to-metal charge transfer (LMCT) from the phenolate oxygen to an empty d orbital of vanadium. As vanadium(V) complexes have $3d^0$ configuration, d → d bands are not expected. There is, however, a strong band at ca. 600 nm for the oxovanadium(V)−benzohydroxamato complexes **6** and **11**, which we assigned to an LMCT originating from the lone pair in a p orbital on the hydroxamato oxygen into an empty d orbital of the vanadium ion. For these complexes, additional bands also appear in the UV region. In vanadium(IV) complexes, broad, unresolved d → d bands are present.

^{1}H, ^{13}C, and ^{51}V NMR Spectral Studies. The coordinating modes of the ligands were confirmed by recording ^{1}H NMR spectra of the ligands and selected complexes, i.e., those which are soluble in suitable solvents. The spectral data are presented in the Experimental Section. Both ligands show a broad signal at 12.9 (**I**) and 13.2 ppm (**II**) due to the phenolic OH. The absence of this signal in the complexes is in conformity with the coordination of the phenolate oxygen to vanadium. A significant downfield shift ($\Delta\delta$ = 0.15−0.26 ppm) of the azomethine (−CH═N−) proton signal in the complexes with respect to the corresponding ligands demonstrates the coordination of the azomethine nitrogen atom. The signals due to the NH group could not be located in the δ = 0−15 ppm region, neither in the spectra of the ligands nor in the complexes. Aromatic and CH_2 protons of

(25) (a) Westland, A. D.; Haque, F.; Bouchard, J.-M. *Inorg. Chem.* **1980**, **19**, 2255−2259. (b) Casný, M.; Rehder, D. *Dalton Trans.* **2004**, 839−846. (c) Sivák, M.; Mad'orová, M.; Taatiersky, J. Marek, J. *Eur. J. Inorg. Chem.* **2003**, 2075−2081.

(26) Nakamoto, K. *Infrared and Raman Spectra of Inorganic and Coordination Compounds*, 3rd Ed.; John Wiley and Sons: New York, 1978; p 241.

(27) (a) Smith, T. S., II; LoBrutto, R.; Pecoraro, V. L., *Coord. Chem. Rev.* **2002**, *228*, 1−18. (b) Garribba, E.; Lodyga-Chruscinska, E.; Micera, G.; Panzanelli, A.; Sanna, D. *Eur. J. Inorg. Chem.* **2005**, 1369−1382.

(28) Tasiopoulos, A. J.; Troganis, A. N.; Evangelou, A.; Raptopoulou, C. P.; Terzis, A.; Deligiannakis, Y.; Kabanos, T. A. *Chem. Eur. J.* **1999**, *5*, 910−921.

(29) Saladino, A. C.; Larsen, S. C., *J. Phys. Chem. A* **2002**, *106*, 10444−10451.

Table 5. ^{13}C NMR Spectroscopic Data

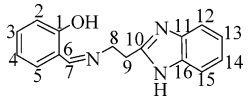

compound[a]	C1	C7	C10	C8	C9	C11	C16	C2−C6, C12−C15
Hsal-ambmz **I**	165.6	162.0	143.9	58.0		134.1	135.1	118.3, 120.7, 121.4, 123.3, 129.4
Hsal-aebmz **II**	166.3	160.4	152.7	56.3	30.1	131.5	132.2	116.3, 118.3, 118.5, 121.1
[VO_2(sal-aebmz)] **8**	168.4	166.0	165.0	62.2	27.3	133.6	133.9	116.8, 118.9, 120.4, 121.1, 123.5, 135.3
($\delta\Delta$)	(2.1)	(5.6)	(12.3)					
[VO(bha)(sal-aebmz)] **11**	168.2	166.8	165.8	57.0	30.7	132.3	132.1	111.7, 117.4, 117.6, 118.8, 120.9, 123.0, 128.1,
($\delta\Delta$)	(1.9)	(6.4)	(13.1)					128.3, 130.7, 133.7, 135.5, 140.1, 154.2

[a] For atom labeling, see scheme above.

the ligands, as well as complexes, appear well within the expected range.

We have also recorded ^{13}C NMR spectra of the ligands and some selected complexes, where solubility permitted. Table 5 contains spectral data along with the assignment of characteristic peaks and coordination induced shifts $\Delta\delta = \delta$(complex) $- \delta$(ligand) of the signals for the carbon atoms in the vicinity of coordinating functions. Large $\Delta\delta$ values for the carbon atoms attached to the phenolic oxygen (C1), azomethine nitrogen (C7), and ring nitrogen (C10) suggest coordination of these atoms.[30] Complex **11** exhibits additional signals in the aromatic region due to the coordinated benzohydroxamato ligand.

The ^{51}V NMR spectral data of the complexes **2**, **4**, and **8** show one strong resonance in the range $\delta = -540.3$ to -567.8 ppm, expected values for dioxovanadium(V) complexes having a mixed O/N donor set.[31] The existence of one strong low-field resonance at $\delta = -71.2$ ppm in **11** reflects the effective charge transfer from the noninnocent benzohydroxamato ligand to the vanadium(V) center.[23] In addition, **11** displays a very weak signal at $\delta = -547.2$ ppm, which belongs to the dioxovanadium(V) species **8**, apparently formed by partial decomposition of **11**. The intensity of this absorption increases with time at the expense of that of the hydroxamto complex (see also the UV−vis section). All of these resonances are somewhat broadened due to quadrupolar interaction (^{51}V: nuclear spin = 7/2, quadrupole moment = -0.05×10^{-28} m^2); with line widths at half-height approximately 200 Hz.[32]

Reactivity of [VO(acac)(sal-aebmz)], [VO(sal-aebmz)$_2$], and [VO_2(sal-aebmz)] toward HCl. Solutions of **7** and **10** in methanol are sensitive toward HCl, as monitored by electronic absorption spectroscopy. Addition of HCl dissolved in methanol to a methanolic solution of **7** results in a reduction in intensity of the 382 nm band, while the shoulder band at 322 nm slowly gains intensity; Figure 5. The intensities of the other bands appearing in the UV region go down (not shown), maintaining their position; a weak shoulder appearing at ca. 700 nm maintains its intensity. The

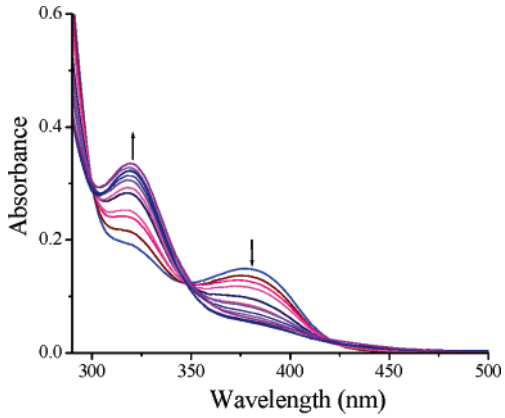

Figure 5. Titration of **7** with HCl in MeOH. The spectra were recorded after successive addition of 1-drop portions of HCl to 10 mL of ca. 10^{-4} M solution of **7**.

reaction can be reversed by treatment with KOH dissolved in methanol. The unchanged 700 nm d → d band and the reversibility of the reaction suggest that protonation of the benzimidazole N occurs during titration with HCl.

At least three different sets of electronic spectral patterns were observed during titration of ca. 10^{-3} M methanolic solution of **10** with very dilute HCl in methanol. The region mainly sensitive to observe these changes is between 300 and 450 nm. In the first set presented in Figure 6, top, the band at 378 nm loses intensity while the band at 321 nm gains intensity. Further addition of HCl causes a considerable reduction in intensity of the 321 nm band, followed by the appearance of a weak band (Figure 6, middle), while position and intensity of the 378 nm band remain constant. Figure 6, bottom, shows the generation of a third species on addition of further HCl, where the 379 nm band slowly shifts to 371 nm with a slight decrease in intensity, while the 318 nm band slowly moves to 325 nm, along with a slight broadening and increase in intensity.

The first step reflects the protonation of the ring nitrogen of the dangling benzimidazole, while the second step possibly is due to protonation of the benzimidazole NH of the coordinated benzimidazole. This interpretation is reasonable, as the spectral patterns corresponding to both protonation steps are reversible on treatment with the methanolic KOH. Our suggestion differs from that of Pecoraro et al.[9] for the complex [VO(sal-im)$_2$], where reversible breaking of the V−N(imidazole) bond has been proposed. Breaking of the V−N(azomethine) bond on addition of 1 equiv of acid has been suggested on the basis of the three-pulse ESEEM

(30) Keramidas, A. D.; Papaioannou, A. B.; Vlahos, A.; Kabanos, T. A.; Bonas, G.; Makriyannis, A.; Rapropoulou, C. P.; Terzis, A. *Inorg. Chem.* **1996**, *35*, 357−367.
(31) Rehder, D.; Weidemann, C.; Duch, A.; Priebsch, W. *Inorg. Chem.* **1988**, *27*, 584−587.
(32) Rehder, D.; In *Transition Metal Nuclear Magnetic Resonance*; Pregosin, P. S., Ed.; Elsevier: New York, 1991; pp 1−58.

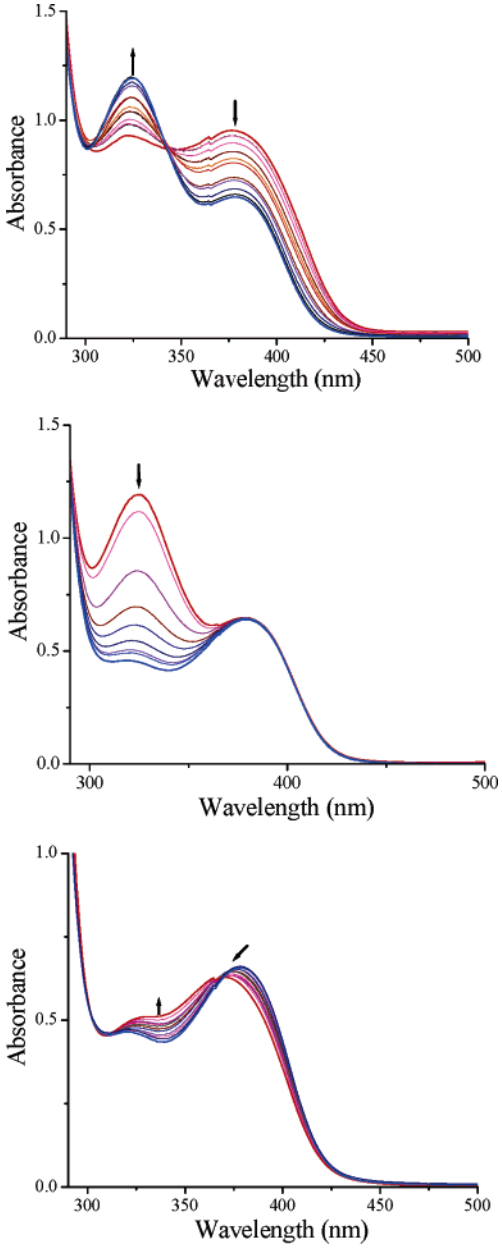

Figure 6. Titration of $[VO(sal\text{-}aebmz)_2]$ **(10)** with HCl. The spectra were recorded after successive addition of 1-drop portions of HCl to 10 mL of ca. 10^{-3} M solution of **10** in MeOH.

spectrum of [VO(acac)(sal-im)].[10] The presence of an isosbestic point at 369 nm in the third set of the titration of **10** may be due to V−N bond breaking through protonation; this step is not completely reversible.

At least two sets of spectral patterns were observed, as shown in Figure 7, upon addition of methanolic HCl to a solution of **8**. The band at 405 nm shows a slight broadening with a decrease in intensity (inset in Figure 7, top), while the band at 313 nm registers no change in intensity. The band at 252 nm remains constant with an increase in intensity, the 273 nm band shifts to 276 nm, with increase in intensity, while the 281 nm band exhibits a gradual shift toward 280 nm and decreases in intensity. Addition of more HCl results in a considerable change in bands position (Figure 7, bottom). Here, the 252 nm band shifts to 255 nm

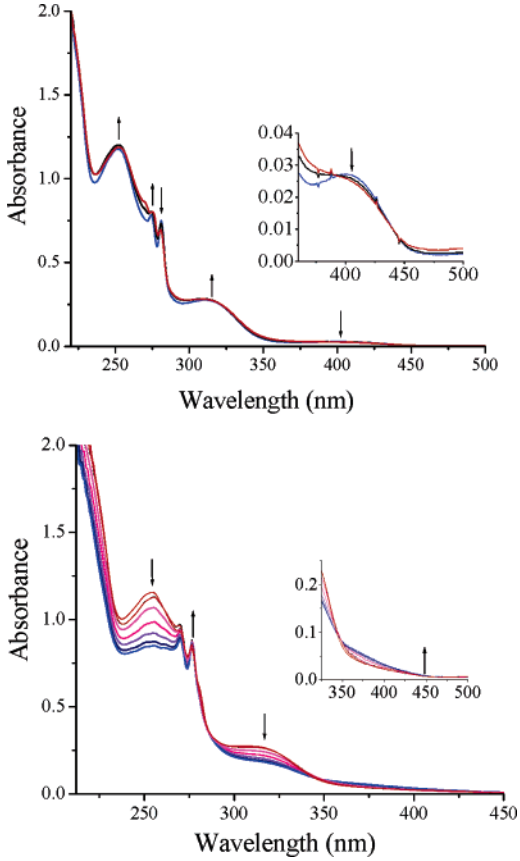

Figure 7. Titration of $[VO_2(sal\text{-}aebmz)]$ **(8)** with HCl in MeOH. The spectra were recorded after successive addition of 1-drop portions of HCl to 10 mL of ca. 10^{-4} M solution of **8**.

with a slight decrease in intensity, while the 276 and 280 nm bands shift to 270 and 276 nm, respectively, along with a slight increase in intensity. The band at 313 nm remains unchanged. Addition of further HCl causes a decrease in intensity of the 313 and 255 nm bands along with broadening. The intensity of the 270 nm band decreases, while that of the 276 nm increases; both bands remain in their positions. We interpret these spectral changes in terms of the formation of an oxohydroxo complex of composition $[VO(OH)(sal\text{-}aebmz)]^{2+}$ via $[VO_2(sal\text{-}aebmzH)]^{+}$, eq 8.

$$[VO_2(sal\text{-}aebmz)] \xrightarrow{H^+} [VO_2(sal\text{-}aebmzH)]^{+} \xrightarrow{H^+} [VO(OH)(sal\text{-}aebmzH)]^{2+} \quad (8)$$

The solution acquired the original spectral pattern upon addition of a methanolic solution of KOH; the reaction is thus reversible. This reversibility is an important observation in the context of the active-site structure and the catalytic activity of vanadate-dependent haloperoxidases, for which a hydroxo ligand at the vanadium center has been made plausible on the basis of X-ray diffraction data.[33,34] We have previously demonstrated the generation of oxo-hydroxovanadium complexes upon acidification of $[K(H_2O)_2][VO_2(pydx\text{-}inh)]$ (H_2pydx-inh = Schiff base derived from salicylaldehyde

(33) Messerschmidt, A.; Prade, L.; Wever, R. *Biol. Chem.* **1997**, *378*, 309−315.
(34) Macedo-Ribeiro, S.; Hemrika, W.; Renirie, R.; Wever, R.; Messerschmidt, A. *J. Biol. Inorg. Chem.* **1999**, *4*, 209−219.

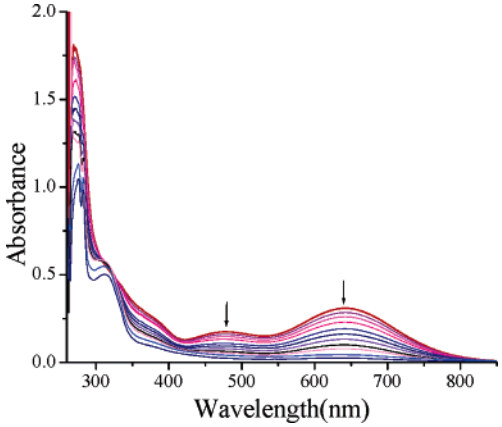

Figure 8. Decomposition of [VO(bha)(sal-aebmz)] (**11**) in 5 mL of DMSO after addition of 2 drops of water as a function of time.

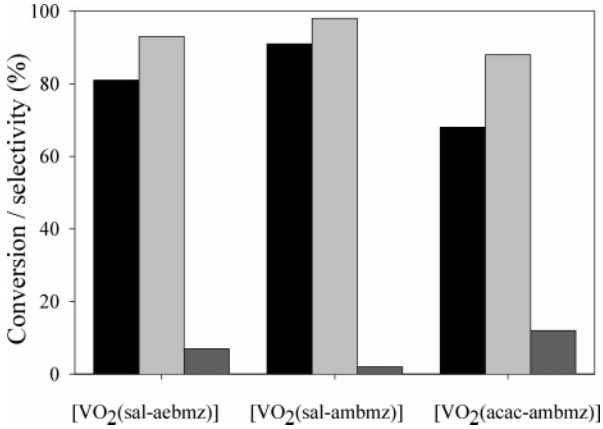

Figure 9. Bar diagram showing the percent conversion (black) of methyl phenyl sulfide and the selectivity with respect to sulfoxide (light gray) and sulfone (dark gray).

and isonicotinic acid hydrazide).[14e] An oxo-hydroxo complex, $[VO(OH)(LH)]^+$ (where LH = *N*-{(*o*-hydroxyphenyl)-methyl}-*N*′-(2-hydroxyethyl)ethylenediamine)[35] has been reported to form from a dinuclear dioxovanadium(V) precursor in a similar manner. $[V^{V}O(OH)(8\text{-oxyquinolinate})_2]$[36] and $[V^{IV}O(OH)Tp(H_2O)]$ [Tp = tris(3,5-diisopropyl-1-pyrazolyl)-borate][37] have been characterized in the solid state.

Stability Studies. As already evidenced by the ^{51}V NMR, complexes **6** and **11** slowly decompose in DMF or DMSO into dioxo species. The decomposition of **6** and **11** into their corresponding dioxovanadium(V) complexes with the loss of the bidentate benzohydroxamate(2−) was also established by electronic absorption spectroscopic studies in DMSO. This conversion is rather slow and takes about 20 h. Addition of a few drops of water accelerates this conversion, leading to completion within 3 h, as shown in Figure 8 for **11**. During this period, a gradual loss in intensity of the LMCT bands at 480 and 643 nm, which is due to coordinated benzohydroxamate, and finally their disappearance was observed. The final spectrum takes the pattern of the dioxovanadium(V) complex **8**. Complex **6** behaves correspondingly. Equation 9 represents the decomposition reaction.

$$[VO(bha)(sal\text{-}aebmz)] + H_2O \rightarrow [VO_2(sal\text{-}aebmz)] + H_2bha \quad (9)$$

Catalytic Activity Studies. As vanadate-dependent haloperoxidases catalyze the oxidation by H_2O_2 of sulfides (thioethers) to sulfoxides and further to sulfones,[6,38] we have also tested the catalytic potential of complexes **2**, **4**, and **8** to mimic the sulfide-peroxidase activity of the enzyme. The oxidation of methyl phenyl sulfide gave a mixture of methyl phenyl sulfoxide and methyl phenyl sulfone (Scheme 3) with a maximum conversion of 91% (with **4**), 81% (**8**), and 68% (**2**) and a selectivity with respect to the major product (the sulfoxide) of 98% (**4**), 93% (**8**), and 88% (**2**). About 3 h were required to acquire the steady state with all the complexes. A blank reaction under similar conditions resulted in 37% conversion of methyl phenyl sulfide, with the percent selectivity for sulfoxide =69.3 and sulfone =30.7. Thus, these complexes not only enhance the percent conversion of substrate, they also improve the selectivity for sulfoxide. The results are presented in Figure 9 in the form of a bar diagram. The turnover rates (mol of product/mol of catalyst h^{-1}) are 28 for **2**, 30 for **4**, and 31 for **8**.

Scheme 3

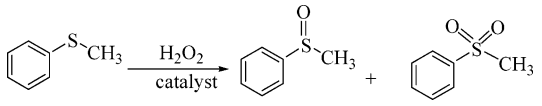

Scheme 4

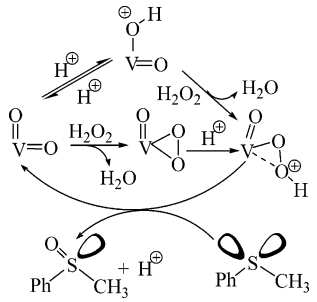

The sulfur atom of methyl phenyl sulfide is electron rich and undergoes electrophilic oxidation giving sulfoxide. As the dioxovanadium(V) complexes **2**, **4**, and **8** are able to generate peroxo species $[VO(O_2)(L)]$ (LH = ligands **I** and **II**) on treatment with H_2O_2, an intermediate peroxo complex is likely to form followed by a hydroperoxovanadium(V) complex in the presence of H^+, enhancing the electrophilicity of the peroxo intermediate.[39,40] The peroxide thus activated is subjected to a nucleophilic attack by the sulfide, as shown in the catalytic cycle proposed in Scheme 4.

Oxidation of Styrene. Complexes **2**, **4**, and **8** were also found to be suitable for the catalytic oxidation of styrene.

(35) Colpas, G. J.; Hamstra, B. J.; Kampf, J. W.; Pecoraro, V. L. *Inorg. Chem.* **1994**, *33*, 4669−4675.
(36) Giacomelli, A.; Floriani, C.; De Souza Duarte, A. O.; Chiesi-Villa, A.; Guastino, C. *Inorg. Chem.* **1982**, *21*, 3310−3316.
(37) Kosugi, M.; Hikichi, S.; Akita, V.; Moro-oka, Y. *Inorg. Chem.* **1999**, *38*, 2567−2578.
(38) (a) Bolm, C.; Bienewald, F. *Angew. Chem.* **1995**, *34*, 2883−2885. (b) Santoni, G.; Licini, G.; Rehder, D. *Chem. Eur. J.* **2003**, *9*, 4700−4708.
(39) Zampella, G.; Fantucci, P.; Pecorao, V. L.; De Gioia, L. *J. Am. Chem. Soc.* **2005**, *127*, 953−960.
(40) Smith, T. S., II; Pecoraro, V. L. *Inorg. Chem.* **2002**, *41*, 6754−6760.

Scheme 5

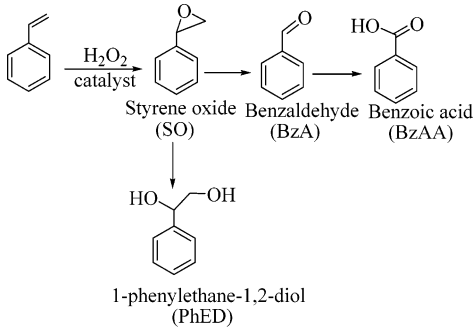

The major oxidation products obtained are styrene oxide, benzaldehyde, benzoic acid, and 1-phenylethane-1,2-diol; see Scheme 5. Epoxidations of alkenes, using model complexes of VHPOs, have been reported previously.[41]

To obtain maximum conversion, we have varied the concentration of the oxidant, using **4** as a representative catalyst under the following operating conditions: styrene (0.51 g, 5 mmol), catalyst (20 mg), temperature (80 °C), acetonitrile (25 mL), and aqueous 30% H_2O_2 (0.5:1, 1:1, 2:1, 3:1, and 4:1 (H_2O_2/styrene) molar ratios). The results are presented in Figure 10. At a 1:1 H_2O_2 ratio, the conversion is 42% in 6 h of contact time. Increasing the ratio to 2:1 increases the conversion to 55%. This conversion could only be improved by about 2−3% upon further increasing the H_2O_2/styrene ratio. Increasing the ratio results in a reduction of the selectivity for styreneoxide from 21% to 4% and an increase in selectivity for benzaldehyde from 64% to 80%. The dilution of the reaction mixture with water on addition of larger amounts of H_2O_2 at higher molar ratios may be responsible for the leveling out of the % conversion.

Under the optimized reaction conditions (i.e., 5 mmol of styrene, 10 mmol of aqueous 30% H_2O_2, 20 mg of catalyst, 25 mL of acetonitrile, 80 °C), complexes **2** and **8** gave 51% and 59% conversion, respectively. Table 6 summarizes the percentage conversion of styrene, the turnover rates, and the selectivities for the various reaction products. All of the catalysts are more selective toward benzaldehyde (74−90%), while selectivity for styrene oxide, an expected product, is rather low (5.5−11%). Due to the strong oxidizing nature of H_2O_2, the styrene oxide formed in the first step by epoxidation is mainly converted into benzaldehyde via the intermediate hydroperoxistyrene. Benzaldehyde formation may also be facilitated by direct oxidative cleavage of the styrene side-chain double bond via a radical mechanism.[42] Water present in H_2O_2 is probably responsibly for the hydrolysis of styrene oxide to form 1-phenylethane-1,2-diol to some extent. Formation of other products, e.g., benzoic acid through oxidation of benzaldehyde, is extremely slow.

Using *tert*-butyl hydroperoxide (TBHP) under optimized reaction conditions (5 mmol of styrene, 10 mmol of aqueous 70% TBHP, 20 mg of catalyst, 25 mL of acetonitrile, 80 °C), the performance of the catalysts toward the conversion of styrene follows the order **8** (35%) > **4**(31%) > **2**(20%),

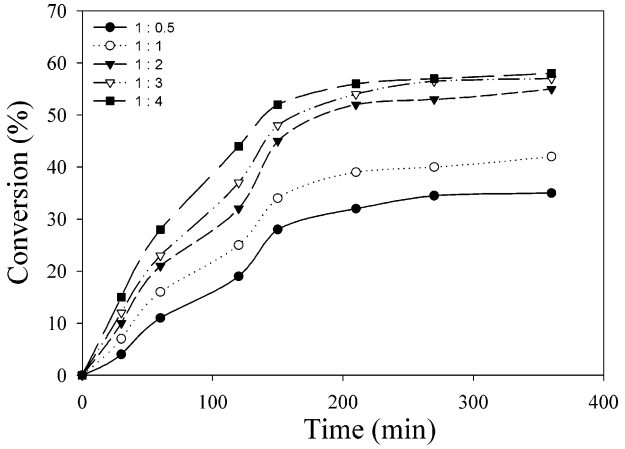

Figure 10. Effect of ratio H_2O_2/styrene on the conversion of styrene. Conditions: styrene (0.51 g, 5 mmol), catalyst **4** (20 mg), temperature (80 °C), CH_3CN (25 mL).

Table 6. Percentage Conversion of Styrene and Selectivity for Various Oxidation Products after 6 h of Reaction Time

				product selectivity			
catalyst	oxidant	conv. (%)	TOF h^{-1}	BzA[a]	SO[b]	BzAA[c]	PhED[d]
2	H_2O_2	51	8.5	90	5.5	0.5	4
4	H_2O_2	55	7.6	74	11	9	6
8	H_2O_2	59	6.6	82	10	5	3
2	TBHP	20	2.6	52	47	1	-
4	TBHP	31	4.3	50	43	5	2
8	TBHP	35	5.1	53	37	8	2

[a] Styrene oxide. [b] Benzaldehyde. [c] Benzoic acid. [d] 1-Phenylethane-1,2-diol.

Table 6. Although the conversion of styrene is low with TBHP, the selectivity for styrene oxide is much better (37−47%) than in the case of H_2O_2, while the yield of benzaldehyde goes down considerably.

Conclusions

The active center of VHPO is constituted by vanadate(V) covalently linked to the imidazole moiety of a histitine side-chain of the protein. Vanadium is in a trigonal-bipyramidal environment, with the imidazole N and an HO− in the axial positions.[2−4] By using Schiff bases containing the benzimidazole (bmz) moiety, we have prepared and characterized a variety of dioxovanadium(V) and oxovanadium(IV) complexes, at least two of which, the dioxovanadium(V) complexes **2** and **8**, can be considered to be structural models of VHPO. These two complexes attain the geometry of a trigonal bipyramid, distorted toward the square pyramid. The τ parameters amount to 0.71 and 0.60, and the bzm-N and RO $^-$ of the acac/sal moiety are in the axis. The model character extends to functional similarities, in that complexes **2** and **8** (and **4**) also model the sulfideperoxidase activity[43] of VHPO. In addition, these complexes catalyze the oxidative conversion, by H_2O_2, of styrene to styrene oxide and successive products derived from styrene oxide.

(41) Bryliakov, K.P.; Talsi, E. P.; Kühn, T.; Bolm, C. *New. J. Chem.* **2003**, *27*, 609−614.
(42) Hulea, V.; Dumitriu, E. *Appl. Catal., A* **2004**, *277*, 99−106.
(43) Andersson, M. A.; Allenmark, S. G., *Tetrahedron* **1998**, *54*, 15293−15304. (b) ten Brink, H. B.; Holland, H. L.; Schoemaker, H. E.; van Lingen, H.; Wever, R. *Tetrahedron: Asymmetry* **1999**, *10*, 4563−4572.

The oxovanadium(IV) complexes of the general formula [VO(co-ligand)(Schiff-base)] (co-ligand = acac, η^2-(sal-aebmz) or sulfate) can be considered to model the reduced, inactive form of VHPO, for which a coordination number of six with participation of two nitrogen functions (from His) has been proposed on the basis of XAS/EXAFS,[44] as well as EPR and ESEEM,[45,46] data.

The complex **8** can be converted, by treatment with H_2O_2, to the peroxo complex **12** and thus to an intermediate[33] in the catalytic cycle representing the activity of VHPO. During turnover, the axial oxo/hydroxo ligand, as well as the pseudo-axial peroxo group[39] of the peroxo intermediate, become reversibly protonated. This protonation has been proposed to be mediated by an active-site amino acid such as lysine and/or (distal) histidine. We present here model studies for this situation by protonating and deprotonating complex **8**, revealing protonation of the bmz moiety in a first step and one of the oxo to a hydroxo group in a second protonation step.

(44) Arber, J. M.; deBoer, E.; Garner, C. D.; Hasnain, S. S.; Wever, R.; *Biochemistry* **1989**, *28*, 7968−7973.
(45) deBoer, E.; Boon, K.; Wever, R. *Biochemistry* **1988**, *27*, 1629−1635.
(46) Hamstra, B. J.; Houseman, A. L. P.; Colpas, G. J.; Kampf, J. W.; LoBrutto, R.; Frasch, W. D.; Pecoraro, V. L. *Inorg. Chem.* **1997**, *36*, 4866−4874.

Acknowledgment. M.R.M. and A.K. thank the Council of Scientific and Industrial Research, New Delhi (Grant No. 01(1826)/02/EMR-II) for financial assistant. We also acknowledge C, H, N, and S analyses carried out by SAIC, Central Drug Research Institute, Lucknow, India. The project was further supported, in part, by the Deutsche Forschungsgemeinschaft (Grant No. RE 432-20-1).

IC0604922